



## CareRAMM Final (Public) Summary Report

Proposal full title: Carbon Resistive Random Access Memory Materials

Proposal acronym: **CareRAMM**

Type of funding scheme: Collaborative Project: (i) Small or medium-scale focused research project

Work programme: NMP.2012.2.2-2 'Materials for data storage'

Coordinator: Professor C David Wright  
([david.wright@exeter.ac.uk](mailto:david.wright@exeter.ac.uk))

# Contents

<b>Introduction to CareRAMM .....</b>	<b>3</b>
<b>Summary of the project results.....</b>	<b>5</b>
<b>Carbon materials for next-generation data storage .....</b>	<b>5</b>
<b>Resistive switching in nanoscale amorphous carbon memory devices .....</b>	<b>7</b>
<b>Understanding the resistive switching process in amorphous carbon using atomistic simulations .....</b>	<b>8</b>
<b>Resistive switching in graphene-oxide memory devices .....</b>	<b>10</b>
<b>Resistance switching mechanisms in graphene-oxide.....</b>	<b>11</b>
<b>Technology Readiness Levels .....</b>	<b>12</b>

# Introduction to CareRAMM – Carbon Resistive Random Access Memory Materials

An FP7 NMP Project led by the University of Exeter and in collaboration with IBM Research Zurich, RWTH-Aachen, University of Cambridge and ISSP-Sofia

There is currently an 'explosion' in data storage requirements reflecting the fact that ICT applications and digital devices are found in all aspects of our daily life, from business to security to medicine to transport to education to leisure etc.. However, current data storage technologies are facing technological barriers to progress in terms of achievable storage densities, power consumption and data rates (e.g. scaling limits in CMOS Flash memories, super-paramagnetic limits in magnetic disk storage). In this context the time is ripe for intensive research and development of alternative data storage materials and concepts.

The increasingly important flexible electronics sector is also not one that is easily addressed using currently available memory materials concepts. The global market for flexible, printed and thin-film electronics is currently estimated to be around \$5 billion, but predicted to grow enormously to over \$60 billion by 2022. A key element of virtually all modern electronic systems is memory and for flexible electronics applications, memories capable of implementation in a flexible format are thus essential.

It is in this context that carbon materials offer an exciting route to the realisation of future generations of high-performance, cost-effective and environmentally friendly non-volatile data storage, suited to both 'conventional' and flexible electronics applications. Scalability to the molecular level, sub-nanosecond switching time, ultra-low power operation, environmental stability, environmental friendliness, simple memory structures, advanced functionality, cost-effectiveness and compatibility with CMOS processing are all features readily provided by carbon-based data storage materials. In the form of graphene-based materials, carbon also offers a particularly attractive route to the provision of memory formats well-suited to the increasingly important flexible electronics arena. Graphene can also provide an extremely versatile electrode material for use in memory structures.

In the CareRAMM project we focus on the exploration and development of next-generation data storage/memory materials via two main carbon-based routes, namely:

- i. thin films of ( $sp^3$ -rich) amorphous carbon (a-C) for the provision of high-performance non-volatile memories
- ii. graphene-based materials in the form of graphene-oxide (GO) for the provision of non-volatile memories which are additionally suited to flexible electronics applications.

The non-volatile storage mechanism in these materials that we investigate involves electrical modification of electrical conductivity, commonly referred to as 'resistive switching'. The exact physical mechanism responsible for this resistive switching in carbon materials was not, before the CareRAMM project started, clear, with  $sp^2$  filamentation,  $sp^2$  clustering, metal filamentation and interfacial redox reactions all being implicated in the literature for various material and electrode configurations. The process of  $sp^2$  filamentation involves a bond re-organisation in which 'strands' of relatively high-conductivity  $sp^2$ -bonded carbon form in a

surrounding  $sp^3$  rich 'matrix'. A switching mechanism driven by such a bond-reorganisation process offers exceptional scaling potential, since ultimately it is a localised 'molecular' process. Bond re-organisation can also be a very fast process, so ultra-fast switching in carbon is also a realistic possibility. Pure  $sp^2$  and  $sp^3$  carbon forms (graphite and diamond) are thermodynamically stable, so carbon also has the potential for long and stable data lifetimes. Additional functionality is also an attractive feature of carbon-based memories. For example, by using graphene, specifically in this project graphene oxide (GO), we open up the route for memories on flexible substrates, a key building block to enable the success of flexible electronics. Carbon-based resistive memories should also offer the capability for multi-level storage and 'memristive-like' behaviour, as seen in other resistive memory materials. Multi-level storage allows for the storage of more than one bit per cell, so increasing data storage densities, while memristive-like behaviour can be exploited to provide a remarkable range of signal processing/computing-type operations, including implementing logic, providing synaptic and neuron-like 'mimics', and performing, in a very efficient way, analogue signal processing functions (such as multiply-accumulate operations).

Clearly carbon offers exciting technical capabilities as a data storage and memory material. There are also compelling environmental reasons that make carbon an attractive proposition; it is, for example:

- Non toxic (to persons or the environment)
- Not reliant on rare mineral extraction (and the knock-on environmental problems)
- Expected to have relatively easy 'end of use' disposal/recycling
- Expected to offer low (total) energy of production (compared to other electronics materials)

In summary then, the general aims of the CareRAMM project are to develop advanced carbon-based resistive switching materials, specifically  $sp^3$ -rich a-C films and graphene-oxide films, for next generation non-volatile data storage applications.

## The project team

The CareRAMM project team consisted mainly of the following researchers:

University of Exeter: C D Wright, M M Aziz, A Alexeev, M Barnes, T Bachmann, M F Craciun  
K Lai, V K Nagareddy

University of Cambridge: A C Ferrari, A K Ott, C Dou, S Milana

IBM Zurich: A Sebastian, W Koelmans, F. Zipoli, A. Curioni, E. Eleftheriou

RWTH-Aachen: M Wuttig, A Yatim, O.Cojocar-Mirédin

ISSP-Sofia: T Tsvetkova

## Summary of CareRAMM project results

### Carbon materials for next-generation data storage

Using a filtered cathodic vacuum arc (FCVA) we prepared amorphous carbon films with the desired high  $sp^3$  content (i.e. tetrahedral amorphous carbon (ta-C) films) required for resistive-switching based memories. In the FCVA system an arc is struck between graphite electrodes in vacuum to create a high energetic plasma of carbon ions. Guided by a magnetic field these ions condense as a thin film on the substrate. The deposition process has been fully optimised in CareRAMM for resistive switching applications. ta-C films with thickness below 20nm can be fabricated with a single deposition run, e.g. only one strike of the arc is used. This helps, as we found in CareRAMM, to reduce the switching voltage and switching field. We used Raman spectroscopy to characterise our amorphous carbon films. All carbon materials show characteristic Raman features in their spectrum. One of these features is called the G peak. Multi-wavelength Raman spectroscopy from deep UV (244nm) to red (633nm) has been performed to extract the mechanical properties of our ta-C films. In amorphous carbon the G peak is dispersive with wavelength. By plotting the position of the G peak,  $Pos(G)$ , versus the laser excitation wavelength we can determine the G peak dispersion  $Disp(G)$  by using a linear fit. From the dispersion it is possible to estimate film properties like Young's modulus, density and  $sp^3$  content. Figure 1a) plots  $Pos(G)$  as a function of excitation wavelength for a 10nm thick ta-C film on Si/SiO<sub>2</sub> substrate. The  $sp^3$  content is higher than 60%.

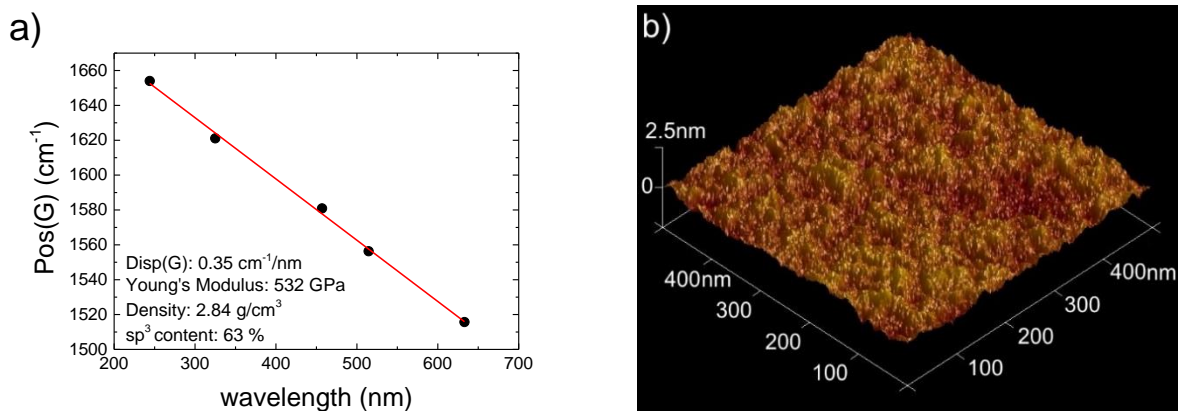


**Figure 1:** a) G peak dispersion of a 10nm thick ta-C film on Si/SiO<sub>2</sub> grown with a single strike of the arc. The inset shows the bonding parameters of the film. b) AFM scan of the same sample. The roughness is 0.233nm.

The roughness of our ta-C films was assessed by atomic force microscopy (AFM). In this process a small, oscillating tip is brought in close proximity to the sample surface and is scanned across the sample resulting in a topographic image of the sample surface. Figure 1b) shows the topography of the 10nm film. This is well below 1nm showing that using a FCVA system ultra-smooth films can be fabricated.

Graphene oxide, GO, also shows promising resistive switching properties. Water based graphene oxide solutions with a concentration of 2mg/ml were prepared, Fig. 2a). These solutions are either filtered to create a thin film or optimised as inks for printing. The filtered

solution leaves a thin GO film on a membrane, Fig. 2b). After dissolving the membrane the GO film can then be transferred on other substrates and further processed to make devices. Fig. 2a) shows a graphene oxide solution in water. This solution is then optimised in terms of wettability and viscosity to meet the requirements for inkjet printing and avoid clogging of the cartridge nozzle, Fig. 2c). The ink was optimised for printing on different substrates, such as Si/SiO<sub>2</sub> as well as flexible substrates such as PET. Fig. 2d) shows a printed test structure of GO on flexible PET substrate. GO films were characterised by Raman spectroscopy to extract the sp<sup>2</sup> cluster size.

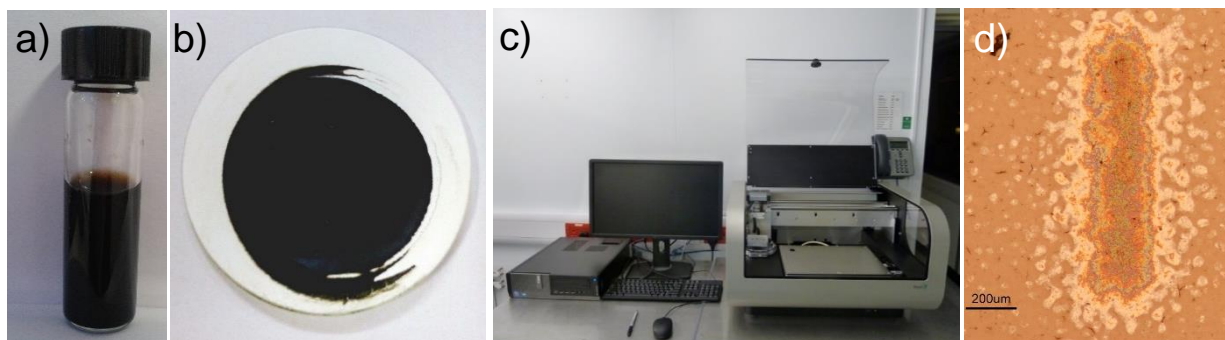


**Figure 2:** a) Aqueous graphene oxide solution. b) Filtered graphene oxide film on membrane. The diameter of the membrane is 2.5cm. c) Inkjet printer. d) Inkjet-printed GO stripe on a flexible PET substrate, scale bar: 200µm.

## Resistive switching in nanoscale amorphous carbon memory devices

In the CareRAMM project we successfully demonstrated reversible resistive memory switching in nanoscale amorphous carbon memory devices. First, we built a memory cell filled with carbon, see Figure 3. The figure also shows a chip filled with hundreds of memory cells that are being accessed by a high-speed measurement probe.

The memory cell has a top and bottom electrode through which electrical pulses are sent to change the state of the memory. We can define a '0' for the low resistance state and a '1' for the high resistance state. In Figure 4, successful memory switching is shown. The state of the cell was here changed more than one hundred times. In addition we showed that the switching process was very fast (few nanoseconds) and potentially of very low energy (few picoJoules). These results show that amorphous carbon offers great potential for the further development of carbon as a memory material.

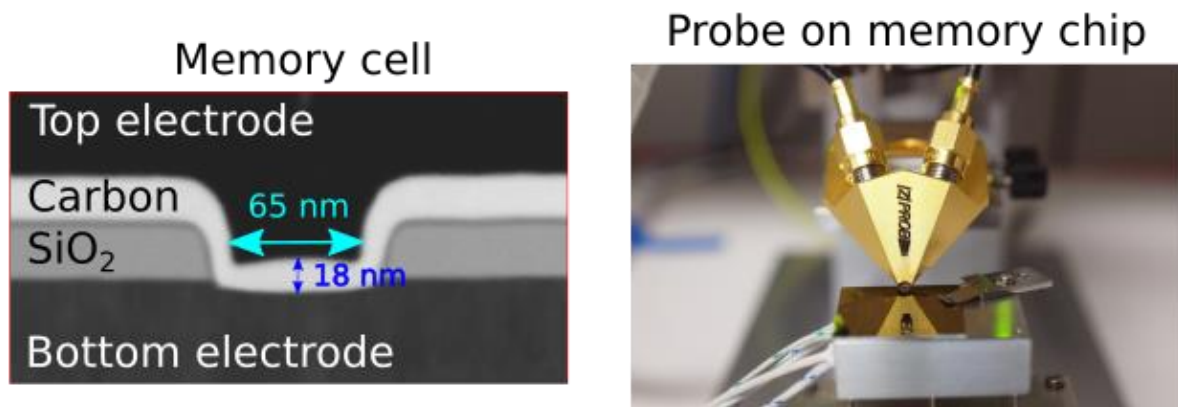


**Figure 3:** Left, a nanoscale memory cell filled with carbon material has been built. Right, a chip with hundreds of these cells is accessed using high-speed measurement probes in an experimental test setup.

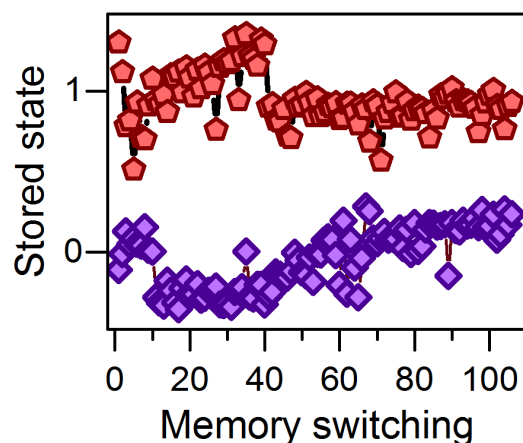


**Figure 4:** Memory switching observed in diamond-like carbon nanoscale cells. More than one hundred cycles in a binary mode are completed.

## Understanding the resistive switching process in amorphous carbon using atomistic simulations

We make combined use of classical molecular-dynamics (MD) simulations and first-principles calculations to elucidate the resistive switching mechanisms in amorphous carbon (a-C). We use classical atomistic simulations at the realistic device sizes to find the optimal set of conditions for reversible resistance switch in a-C and first-principles calculations based on density-functional theory on smaller systems to link the structural and the electronic properties. We develop an original augmented-Tersoff classical potential to model a-C allowing fast MD simulations lasting tens of nanoseconds of systems containing up to two million atoms using box sizes up to  $27 \times 27 \times 18 \text{ nm}^3$  which match the range of thickness of a-C films in the memory device, typically from (5–20) nm.

We simulate the resistance switch produced by the passage of the electric current via the use of multiple thermostats as illustrated in Figure 5. Our model assumes that the main effect of the electric field is to heat the system via an increase of temperature of the atoms forming conducting pathways between the electrodes. In the example of Figure 5, the atoms of the filament are coloured in red. The amount of Joule heat is higher where the resistance is lower, *i.e.* along pathways with higher density of  $sp^2$  atoms. Thus, we enforce a high temperature  $T_H = (1500\text{--}2500) \text{ K}$  to the atoms in this conductive region via a thermostat. Two additional thermostats, set to a low temperature  $T_L = (300\text{--}500) \text{ K}$ , are coupled to the atoms located in the blue and cyan regions in the inset of Figure 5 to take into account the heat dissipated via the electrodes and the surrounding a-C matrix.

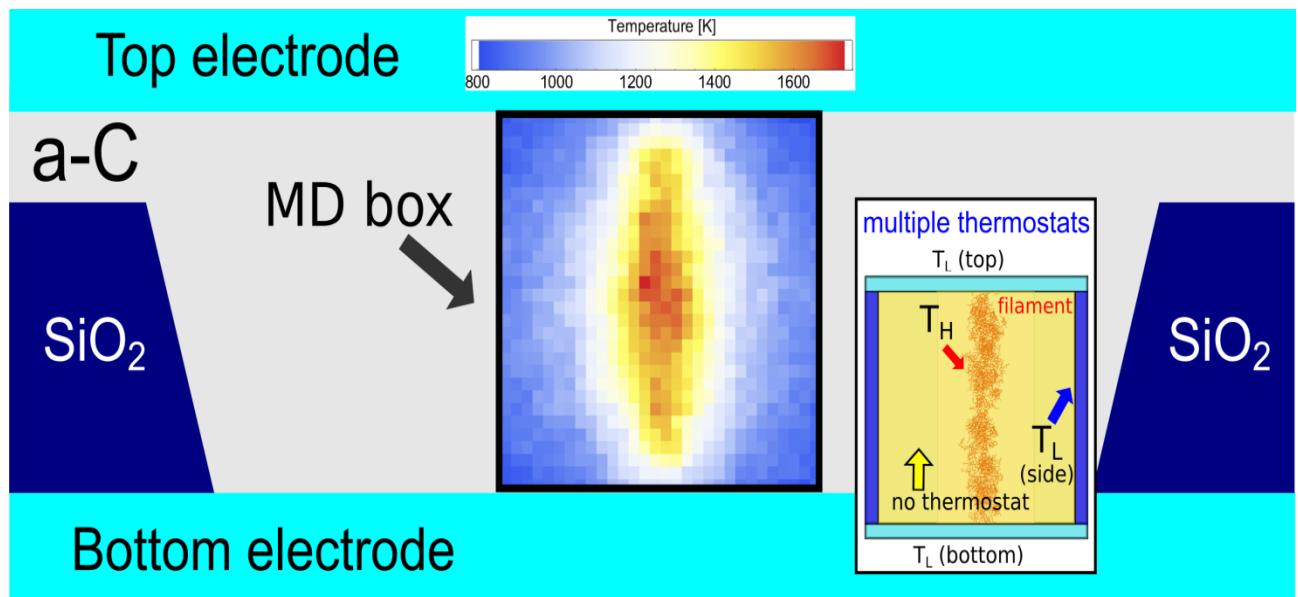


**Figure 5:** Schematic representation of the memory device. Prototypical temperature distribution resulting by the passage of a current through the filament. The inset show the three thermostats used to produce the temperature profile produced by the passage of a current in the device. The colour code is red for the higher  $T$ ,  $T_H$ , and blue for the lower  $T$ ,  $T_L$ , see the inset below.

Assuming that overall the density of reactive region in a-C cannot undergo a substantial change, we simulate the SET and RESET step via constant volume simulations. Our

atomistic simulations show that the SET step from a pristine sample involves re-hybridization of  $sp^3$  atoms in  $sp^2$ . The atomic density, which was uniform in the pristine sample, changes as the re-hybridization occurs. The density decreases in the region at high temperature, in which  $sp^3$  atoms become  $sp^2$ , and where the conductive pathway forms. The amorphous carbon matrix in the vicinity of the hot region accommodates the expansion by increasing its density via re-hybridization of  $sp^2$  atoms in  $sp^3$ . We found that the formation of conductive  $sp^2$  filaments is possible as long as the  $sp^3$  content does not exceed 50 %. At higher  $sp^3$  contents, we observed the growth of  $sp^2$  clusters close to each other and not connected into a single conjugated filament (but still yielding a conductive pathway).

The RESET step occurs via re-hybridization of a few hundred atoms among the few thousands of atoms forming the conductive pathway, which can be either a filament, as illustrated in Figure 6, or a group of clusters close but not connected via conjugated bonds. In the case of Figure 6, this re-hybridization fragments the filament in smaller clusters. In order to compensate the increase of density due to the  $sp^2$  to  $sp^3$  conversion, such  $sp^2$  clusters can grow in the direction orthogonal to the filament via opposite re-hybridization. We found that the re-hybridizations occurring in the RESET step are facilitated by the temperature gradient produced by the heat dissipated via the top and bottom electrodes.

Our atomistic simulations show that this is most likely the mechanism of resistance switch if we assume that the a-C matrix is confined in a region in which the total density cannot vary. The results suggest that a reversible resistance switch is unlikely to occur if the  $sp^3$  content in the whole cell is less than 35 %, because this is too close to the percolation threshold and the cell is conductive pathway cannot be effectively broken by the RESET process. We found that an  $sp^3$  content of about 50% or higher is desirable to limit the extent of the conductive pathways, thus improving reversibility (i.e. making the RESET process easier).

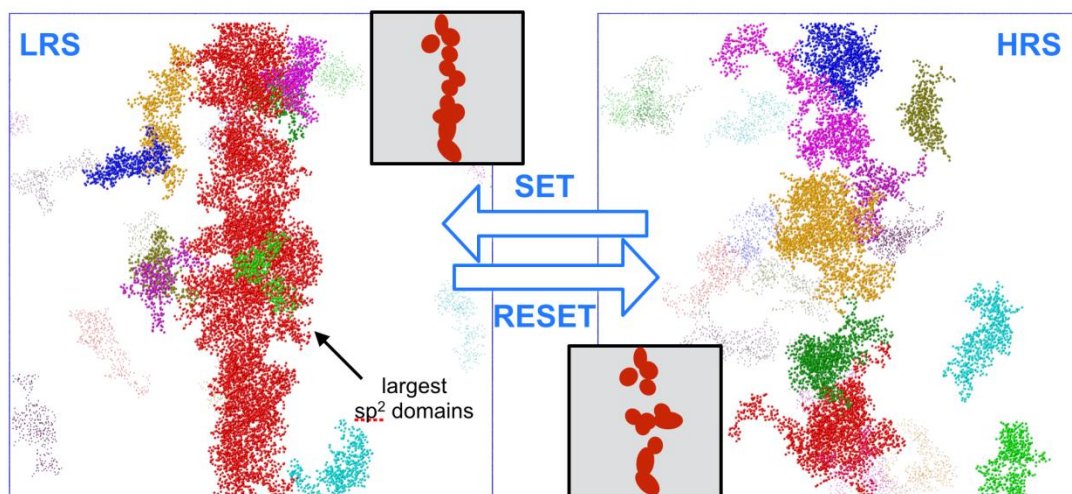


**Figure 6:** Structures of the low resistance state (LRS) and high resistance state (HRS). The larger  $sp^2$  clusters are indicated by different colours. The inset illustrates the structure of the LRS and HRS.

## Resistive switching in graphene-oxide memory devices

In CareRAMM project we have also successfully developed graphene-oxide (GO) based memory devices that can be reliably and repeatedly switched between two resistance states and which are suitable for flexible electronics applications. The devices are formed from thin layers of GO sandwiched between platinum and titanium electrodes, all fabricated on a plastic substrate (see Fig. 7(a)). These GO memory cells were capable of being switched at very high speeds ( $< 10$  ns), being scaled down to very small sizes ( $< 100$  nm) and had excellent switching properties (see Fig. 7(b)).

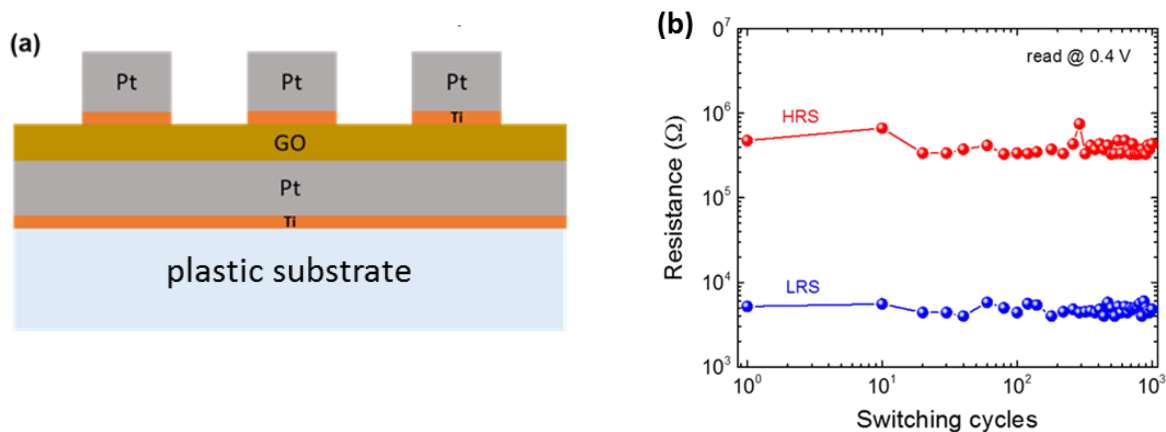


**Figure 7:** GO-based memory device structure (left) and resistive switching properties (right).

The switching mechanism in our GO devices is bipolar, by that we mean that if a positive voltage switches the cell from low to high resistance state, a negative voltage is required to switch it back again (this is different to switching in the a-C memories described earlier which is unipolar). A typical switching curve is shown in Fig. 8(a). Also shown in Fig. 8 is a batch of GO memory devices fabricated on a plastic substrate and undergoing bending tests. We found that our GO memory devices could withstand many bending cycles (many 1000s of cycles) without any significant degradation of performance.

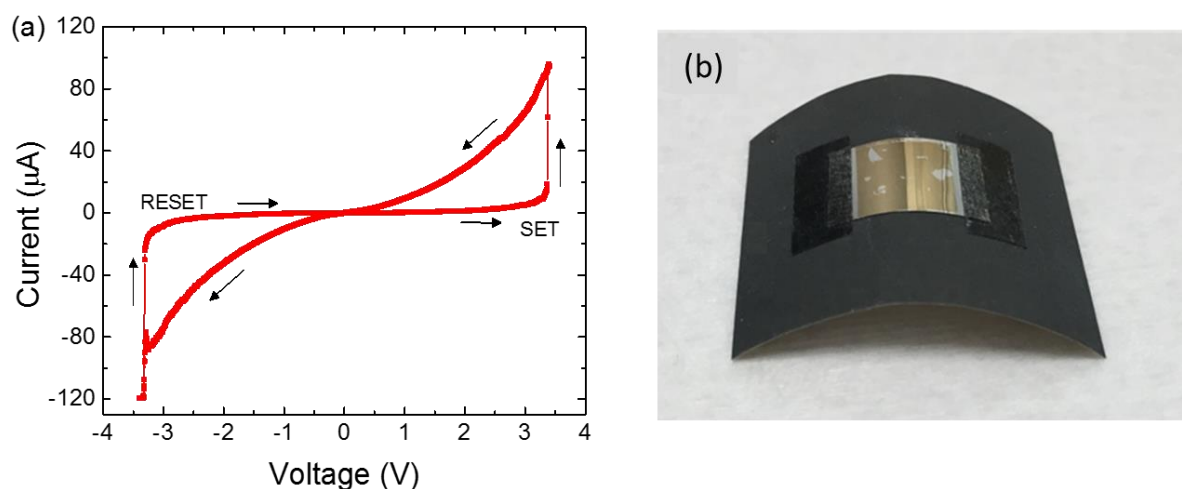


**Figure 8:** Bipolar switching in GO-based memory device (left) and GO-based memories fabricated on plastic substrates and subjected to bending tests (right)

## Resistance switching mechanisms in graphene-oxide

Our experimental studies of resistive switching in the GO-based memory devices described above suggest that switching is driven by a reversible redox (reduction-oxidation) process at the Ti/GO interface. We therefore investigated this hypothesis via first-principles atomistic simulations. Specifically we modelled GO and the Ti/GO interface with structures containing around 600 atoms (we need to limit our study to small systems, because we use density-functional-theory and the computationally expensive hybrid functional PBE0 to find electronic properties). We found (energy) barrier-less irreversible migration of oxygen atoms from GO to the titanium, resulting in an oxidized titanium surface and graphene-oxide layer with a low oxygen content, see Figure 9(a). The energy gain for each O-atom in this case was about (3–5) eV. Other oxygen atoms are more however stable; these O-atoms are part of C=O and O-C-O groups in the plane of graphene; these groups are located in the voids of the graphene-oxide, see Figure 9(b). An activation energy barrier in the order of 1.6 eV is enough to transfer these O-atoms to the titanium. This process is reversible and the energy of the initial and final configuration is relatively similar, see inset in Fig, 9(b). We report also reversible absorption of water molecules from gas phase to the oxidized titanium surface.

These exploratory calculations show that reversible switch may involve only the O-atoms located in the voids of graphene-oxide, which are more stable than the out-of-plane oxygen. Similarly water molecules from the gas phase can reversibly bind to the titanium surface. For these groups, we report reversible transfer from GO to titanium with relatively activation energy barrier of the order of (1–2) eV.

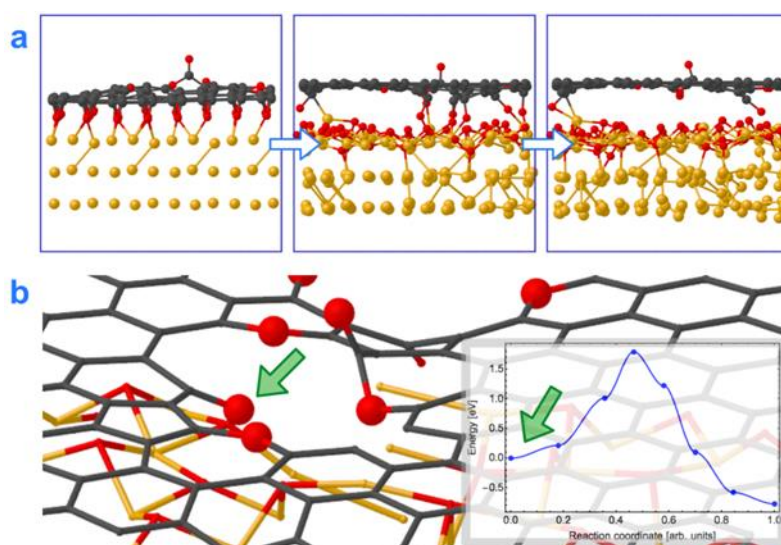


**Figure 9:** (a) Barrier-less oxygen transfer from GO to titanium surface. The colour code is titanium, carbon, and oxygen atoms are depicted in yellow, grey, and red respectively. (b) The atoms indicated with larger spheres are the more stable O-atoms occupying the voids in GO. The transfer of these O-atoms to titanium is a reversible activated processes with energy barrier profile of the order of 1 eV, see inset in (b).

## Technology Readiness Levels

CareRAMM activities were in the main focused around the TRL levels 1 to 3, i.e.

TRL 1 – basic principles observed

TRL 2 – technology concept formulated

TRL 3 – experimental proof of concept

We assess that the TRL levels achieved (by ourselves and others working in the field) at the start of the project in the two main target project areas, i.e.

(i) resistive-switching in thin film amorphous carbon (a-C) materials for non-volatile memory applications, and

(ii) resistive-switching in graphene oxide (GO) thin film materials for non-volatile memory applications (including memories for flexible electronics applications)

were **TRL 2 and TRL 1 respectively**.

**At the end of the project** we assess that the levels achieved by the CareRAMM project were at **TRL 3** in both cases.

In terms of the CareRAMM's originally-stated **measurable project objectives** (listed on page 8 of the DoW), the end of the project status of such objectives is as outlined in the table below (along with the status achieved at the time of the mid-term review):

Technical objective - As stated in DoW	Technical objective - At mid-term review stage (M18)	Technical objective - At end of project (M36)
sub-nanosecond switching (set/reset) times <i>Note – originally envisaged as target only for a-C devices</i>	<i>In a-C devices:</i> 100 ns (set)/ 30 ns (reset)	<i>In a-C devices:</i> 50 ns (set – for rewritable applications) <5 ns (set – for write once applications) <4 ns (RESET)  <i>In GO devices</i> <10 ns (set/reset)
sub-10 nm feature size (switching region) <i>Note – originally envisaged as target only for a-C devices</i>	<i>In a-C devices:</i> (i) 12.5 nm feature size demonstrated in C-AFM (ii) sub-100 nm feature size in device configuration	<i>In a-C devices:</i> (i) sub-10 nm feature size demonstrated in C-AFM (ii) 50 nm feature size in confined-cell device configuration (iii) 10 nm feature size in lateral cell device configuration  <i>In GO devices:</i> < 50 nm cells
sub-10 $\mu$ W write power (~ pJ write energy) <i>Note – originally envisaged as target only for a-C devices</i>	<i>In a-C devices:</i> 1200 $\mu$ W (15 pJ) switching demonstrated	<i>In a-C confined-cell devices:</i> 15 pJ (set - for re-writable applications) < 5 pJ (set - for write once) 3 pJ (reset) <i>In a-Cox devices:</i> 2 pJ (set)

		<p>1 pJ (reset)</p> <p><i>In lateral a-C cells:</i> Sub-<math>\mu</math>W and sub-pJ switching observed!</p> <p><i>In GO devices:</i> &lt; 5 pJ (set/reset)</p>
<p>predicted lifetime of at least 10 years at 100°C for consumer applications</p> <p><i>Note – target only for a-C devices</i></p>	Not yet assessed - planned for 2nd period	<p><i>In a-C confined-cell devices:</i> Retention of &gt; 10,000 s at 85 °C demonstrated. Retention of &gt; 1000 s at 300 °C demonstrated. Predicted lifetime of 10 years at 100°C expected.</p>
<p>predicted lifetime of at least 10 years at 200°C for automotive, aerospace and military applications</p> <p><i>Note – target only for a-C devices</i></p>	Not yet assessed - planned for 2nd period	<p><i>In a-C confined-cell devices:</i> Operating temperatures up to 300°C demonstrated. Retention of over 1000s at 300°C demonstrated. Predicted lifetime at 200C expected to be good – but not quantitatively assessed</p>
demonstration of binary and multi-level storage capability	Not yet assessed - planned for 2nd period	<p><i>In a-C devices:</i> Demonstration of possible 3-level storage (one-and-a-half-bits per cell) in a-C confined-cell.</p> <p><i>In GO devices:</i> Demonstration of excellent 4-level (2 bits per cell) storage, including retention demonstration of each level.</p>
demonstration of memristive-like 'additional functionality'	Not yet assessed - planned for 2nd period	Memristive-like 'additional functionality' demonstrated in a-CO <sub>x</sub> devices (specifically an accumulation property useful for arithmetic and neuronal processing)
demonstration of suitability of GO-based memory for flexible electronics applications	GO device-like structures successfully fabricated on flexible substrates, but re-writability not yet achieved in this format	<p>Excellent performance of GO memories on flexible substrates demonstrated (better than any results reported in literature to date).</p> <p>SET/RESET states stable for &gt; 10,000 bending cycles and high bending radii</p> <p>Endurance (#switching cycles) of over 1000 achieved on flexible substrates.</p>

Overall the CareRAMM project has achieved its original scientific and technological objectives. We have significantly advanced the state-of-the-art in terms of both amorphous carbon and GO based memories, achieving switching speeds and energies better than anything so far reported, as well as successfully fabricating and characterizing the smallest a-C and GO memory devices yet made. We have also advanced the community's scientific understanding of the switching processes at play in such materials and devices, showing (by a combination of ab initio simulation and nanoscale experimental characterization methods) that switching in a-C device (with inert electrodes) is driven by sp<sup>2</sup> filamentation/clustering, while switching in GO devices with Pt/Ti electrodes is driven by redox reactions at the Ti/GO interface.